Quantum model of a solid-state spin qubit: Ni cluster on a silicon surface by the generalized spin Hamiltonian and X-ray absorption spectroscopy investigations

Oleg V. Farberovich [a,b,c], Victoria L. Mazalova [b,*], Alexander V. Soldatov [b]

[a] School of Physics and Astronomy, Beverly and Raymond Sackler Faculty of Exact Sciences, Tel Aviv University, Tel Aviv 69978, Israel
[b] Research Center for Nanoscale Structure of Matter, Southern Federal University, Zorge 5, 344090 Rostov-on-Don, Russia
[c] Voronezh State University, Voronezh 394000, Russia

ARTICLE INFO

ABSTRACT

We present here the quantum model of a Ni solid-state electron spin qubit on a silicon surface with the use of a density-functional scheme for the calculation of the exchange integrals in the non-collinear spin configurations in the generalized spin Hamiltonian (GSH) with the anisotropic exchange coupling parameters linking the nickel ions with a silicon substrate. In this model the interaction of a spin qubit with substrate is considered in GSH at the calculation of exchange integrals J_{ij} of the nanosystem Ni_7–Si in the one-electron approach taking into account chemical bonds of all Si-atoms of a substrate (environment) with atoms of the Ni_7-cluster. The energy pattern was found from the effective GSH Hamiltonian acting in the restricted spin space of the Ni ions by the application of the irreducible tensor operators (ITO) technique. In this paper we offer the model of the quantum solid-state N-spin qubit based on the studying of the spin structure and the spin-dynamics simulations of the 3d-metal Ni clusters on the silicon surface. The solution of the problem of the entanglement between spin states in the N-spin systems is becoming more interesting when considering clusters or molecules with a spectral gap in their density of states. For quantifying the distribution of the entanglement between the individual spin eigenvalues (modes) in the spin structure of the N-spin system we use the density of entanglement (DOE). In this study we have developed and used the advanced high-precision numerical techniques to accurately assess the details of the decoherence process governing the dynamics of the N-spin qubits interacting with a silicon surface. We have studied the Rabi oscillations to evaluate the N-spin qubits system as a function of the time and the magnetic field. We have observed the stabilized Rabi oscillations and have stabilized the quantum dynamical qubit state and Rabi driving after a fixed time (0.327 μs). The comparison of the energy pattern with the anisotropic exchange models conventionally used for the analysis of this system and, with the results of the experimental XANES spectra, shows that our complex investigations provide a good description of the pattern of the spin levels and the spin structures of the nanomagnetic Ni_7 qubit. The results are discussed in the view of the general problem of the solid-state spin qubits and the spin structure of the Ni cluster.

© 2015 Elsevier B.V. All rights reserved.

1. Introduction

The promise of quantum computers to solve classically non-computable problems [1] has generated the great excitement and much research activity in different areas of physics, mathematics and engineering. Various physical systems have been proposed for implementation of quantum bits (qubits) in quantum information processing devices: trapped ions, atoms in QED cavities, magnetic

molecules, etc. Among many candidates, spin-based solid-state systems, such as quantum dots [2,3] or spin centers in host crystals (phosphorus donors in silicon [4], NV centers in diamonds [5,6]), constitute attractive candidates for qubits: these systems are well scalable, can be fabricated and operated by the methods of modern microelectronics, and advanced spin-resonance techniques are well-suited for the efficient quantum state manipulation. Thus, it is not surprising that a large number of leading research groups, both theoretical and experimental, focus their studies on developing and investigating solid-state spin-based qubits. It should be noted that the study of such objects is only at the beginning, as

opposed to molecular systems [7], and is currently more interesting and important for fundamental reasons.

Since the quantum computing technology is being improved and quantum computers with the nontrivial number of N qubits appear feasible in the near future, an application of the quantum computers with $N \geq 2000$ has ripened [8]. The information technologies provide very interesting challenges and an extremely wide playground in which scientists working in materials science, chemistry, physics and nano-fabrication technologies may find stimuli for novel ideas. Curiously, the nanometre scale is the cluster scale. So we may wonder whether, how or simply which functional magnetic clusters can be regarded in some ways as the possible components of the solid-state electron spin qubit, which is the fundamental concept of the quantum computation. Key challenges in building a quantum computer from spin qubits in physical systems are the preparation of arbitrary spin states, implementation of the arbitrary qubit evolution, reading out the qubit states, overcoming of the decoherence and doing all this on a large scale; that is, with a large number of qubits or a spin system of N-qubits (SSNQ) with the definite spin structure. For the purposes of implementing quantum computation, the physical system can be treated as a SSNQ in which the couplings between the qubits can be controlled externally. The concept of a SSNQ can be related to the problem of the quantum spin structure, where the nontrivial applications may exist for computers with a limited number N of a qubits. The precise relationship between the type of the entanglement and the distribution of the coupling strengths in the SSNQ can be strongly dependent on external parameters, such as applied magnetic fields and temperature. In this context, systematic studies of the relationship between the amount and nature of the entanglement and the spin structure of the SSNQ has been pursued in order to identify the optimal spin structures to create specific types of the entanglements [9].

Spins are alternative complementary to charges as degrees of freedom to encode information. Recent examples, like for instance the discovery and application of Giant magnetoresistance in Spintronics, have demonstrated the efficient use of a spins for information technologies [11]. Moreover, spins are intrinsically quantum entities and they have therefore been widely investigated in the field of the quantum-information processing. The cluster nanomagnets of a transition metal are real examples of finite spin-clusters (0D), and therefore they constitute a new benchmark for testing models of the interacting quantum objects. New physics of the cluster magnets feeds hopes of certain prospective applications, and such hopes pose the problem of understanding, improving, or predicting desirable characteristics of these materials. The magnetic transition metal nanostructures on non-magnetic substrates have attracted recently large attention due to their novel and the unusual magnetic properties [12]. The supported clusters experience both the reduction of the local coordination number, as in free clusters, and the interactions with the electronic degrees of freedom of the substrate, as in embedded clusters. The complex magnetic behavior is usually associated with the competition of the several interactions, such as interatomic exchange and bonding interactions, and in some cases the non-collinear effects, which can give rise to the several metastable states close in energy. The ground state can therefore be easily tuned by external action giving rise to the switching between different states [13].

Therefore the goal is ambitious: it is not just a matter to store information in a 3d-metal cluster on a non-magnetic substrate, but we may think to process information with a cluster and then to communicate information at the clusters containing from magnetic 3d-metal atoms on a silicon surface. Among the various candidates for a solid-state qubits, spins have been of the particular interest due to their relative robustness to decoherence compared with other degrees of freedom, such as a charge. The most coherent solid-state systems investigated so far are the spins of well isolated donors in bulk 28Si, which produce coherence times (T2) of up to seconds (extrapolated) for the electron spin and minutes for the nuclear spin, which are comparable to those of a ion trap qubits [10]. The problem of decoherence comprises our main motivation to study the decoherence dynamics of a N-qubits system [14–16]. From the experimental point of view, the coherent transition from a coherent to an incoherent dynamics can be probed by the observation of Rabi oscillations between the quantum states of the spin processing in a static magnetic field [24]. A related problem in the context of the present study is the Rabi oscillations in a SSNQ. Here we suggest for construction of the spin qubit the Ni small clusters on a silicon surface. The stabilization of Rabi oscillations and the maximum of the entanglement were discussed in this SSNQ. In recent years, the entanglement has attracted the attention of many physicists working in the area of quantum mechanics [17–19,24]. This is due to the ongoing research in the area of quantum information [20]. Theoretical studies are also important in the context of spin interactions inside structured reservoirs such as a metal cluster on a nonmagnetic surface. Ni is the unique among the transition-metal adatoms, because its half-filled valence configuration ($3d^8 4s^2$) yields strong interatomic bonding leading to magnetic frustration. We apply our method to the Ni clusters deposited on a Si(111) surface. In the present work we study the entanglement between the spin states in the spin spectrum. In our model, a spin state interacts with the spin structure of the continuum at the temperature interval 0–300 K, and the entanglement properties between the spin states in the spin structure are considered. Using the global entanglement as a measure of the entanglement, we derive a pair of distributions that can be interpreted as the density of entanglement in terms of all the eigenvalue of the spin spectrum. This distribution can be calculated in terms of the spectrum of the spin excitation of the Ni$_7$-cluster on a Si (111)-surface. With these new measures of the entanglement we can study in detail the entanglement between the spin modes in the spin structure. The method developed here, in terms of the entanglement distributions, can also be used when considering various types of the structured reservoirs [22]. The low-lying excited states of a magnetic system are generally described in the of a general spin-Hamiltonian [22,23]. For a magnetic system with many spin sites, this phenomenological Hamiltonian is written as a sum of pair-wise spin exchange interactions between adjacent spin sites in a cluster and a surface.

As the most properties depend on the unique features of the local atomic structure, the diagnostic methods to the control structural parameters, such as the distances between the atoms, with the very high precision are required. In this work, X-Ray Absorption Near-Edge Structure (XANES) spectroscopy was used both to study the adsorption geometry and to get information concerning the electronic properties of the deposited Ni$_7$ clusters [25,26]. XANES spectroscopy is now a powerful tool of investigation of the atomic and electronic structure of different classes of materials in a condensed state. The XANES spectroscopy has essential advantages as compared with other methods of atomic structure analysis. For example, in contrast to X-ray and neutron crystallography, XANES spectroscopy can be used for the investigation of materials without long order in atoms arrangement. Extended X-ray Absorption fine structure (EXAFS) spectroscopy also allows studying the compounds without long order, but it can give only information about the coordination numbers and interatomic distances, while XANES is very sensitive to both the small bond distance and bond angle variations. For example, XANES allows the determination of the interatomic distances with 0.02 Å accuracy as well as the study of bonding angles with the accuracy up to several degrees. Thus, on the basis of XANES

analysis it is possible to determine the full 3D atomic structure of studied materials. Previously, we have used the method of X-ray absorption spectroscopy for a comprehensive study of copper nanoclusters and diluted magnetic semiconductors [25,26]. The knowledge of the properties of nanoclusters made it possible to obtain information on how the transition from the atom or cluster to the solid state can occur. In order to extract the necessary information from the experimental XANES spectra one needs to perform theoretical analysis. In the present research the theoretical XANES spectra were simulated using FEFF9.0 program code [27,28]. FEFF9.0 code is based on the real space full-multiple scattering theory. The code uses the cluster approach for XANES spectral calculations and, therefore (in contrast to program based on the band structure calculations), can be applied for the study of compounds without long order in atom distributions, like clusters. The electronic structure of investigated clusters was analyzed on the basis of the density functional theory (DFT) implemented in the ADF2013 code [29,30].

2. The theoretical approach

We are using here a quantum algorithm with the three distinct steps: the calculation of the magnetic properties for the qubit; encoding a spin wavefunction into the qubits (the spin structure); a spin-dynamics simulating its time evolution. In order to give a theoretical description of a magnetic cluster we exploit the irreducible tensor operator technique [23]. Let us consider a spin cluster of an arbitrary topology formed from an arbitrary number of the magnetic sites, N, with a local spins S_1, S_2,..., S_N which, in general, can have different values. A successive spin coupling scheme is adopted

$$S_1 + S_2 = S^{(2)}, \quad S^{(2)} + S_3 = S^{(3)}, \ldots, S^{(N-1)} + S_N = S, \quad (1)$$

where S represents the complete set of intermediate spin quantum numbers $S^{(k)}$, with $k=1,2,\ldots,N-1$. The eigenstates $|SM\rangle$ of the spin-Hamiltonian are given by the linear combinations of the basis states $|S^{(\mu)}M^{(\mu)}\rangle$:

$$|SM\rangle = \sum_{\mu=1}^{N} \langle c_\mu | SM \rangle |S^{(\mu)}M^{(\mu)}\rangle, \quad (2)$$

$M = -S, \ldots, S$ and the coefficients $\langle c_\mu | SM \rangle$ can be evaluated once the spin-Hamiltonian of the system has been diagonalized. Each term of the spin-Hamiltonian can be rewritten as a combination of the irreducible tensor operators technique [23]. The work [21] focuses on the main physical interactions which determine the spin-Hamiltonian and to rewrite them in terms of the ITO's. The exchange part of the spin-Hamiltonian is introduced

$$\hat{H}_{spin} = \hat{H}_0 + \hat{H}_{BQ} + \hat{H}_{AS} + \hat{H}_{AN}. \quad (3)$$

The first term $\hat{H}_0$ is the Heisenberg Hamiltonian, which represents the isotropic exchange interaction, $\hat{H}_{BQ}$ is the biquadratic exchange Hamiltonian, $\hat{H}_{AS}$ is the antisymmetric exchange Hamiltonian, and $\hat{H}_{AN}$ represents the anisotropic exchange interaction. Conventionally, they can be expressed as follows [21]:

$$\hat{H}_0 = -2 \sum_{i,f} J_{if} \hat{S}_i \hat{S}_f \quad (4)$$

$$\hat{H}_{BQ} = -\sum_{i,f} j_{if} (\hat{S}_i \hat{S}_f)^2 \quad (5)$$

$$\hat{H}_{AS} = \sum_{i,f} \mathbf{G}_{if} [\hat{S}_i \times \hat{S}_f] \quad (6)$$

$$\hat{H}_{AN} = -2 \sum_{i,f} \sum_{\alpha} J_{if}^{\alpha} \hat{S}_i^{\alpha} \hat{S}_f^{\alpha} \quad (7)$$

with $\alpha = x,y,z$.

We can add to the exchange Hamiltonian the term due to the axial single-ion anisotropy:

$$\hat{H}_{ZF} = \sum_i D_i \hat{S}_z^2(i) \quad (8)$$

where J_{if} and J_{if}^{α} are the parameters of the isotropic and anisotropic exchange iterations, j_{if} are the coefficients of the biquadratic exchange iterations, and $\mathbf{G}_{if} = -\mathbf{G}_{fi}$ is the vector of the antisymmetric exchange. The terms of the spin-Hamiltonian above can be written in terms of the ITO's.

In this paper, we use the results of first-principles calculations of the exchange parameters J_{ij}. Here, we introduce the scenario [34] to construct the parameters within the classical spin model that contains the interactions, in principle, up to an arbitrary order. Our development of a non-collinear method is based on semi-relativistic first-principle calculations of the energy in the framework of the density functional theory (DFT) within the linear combination of the atomic orbitals (LCAO) method [35]. We suggested a straightforward approach that allows the direction of the magnetic moment of any atom to be fixed by using only an on-site information [36]. Thus, we can obtain a sufficiently large number of states with different non-collinear magnetic orderings and map them onto an effective spin model by using least-squares methods.

The Heisenberg and biquadratic exchange are the isotropic interactions. In fact, the corresponding Hamiltonians can be described by the rank-0 tensor operators and thus these have the non-zero matrix elements only with states with the same total spin quantum number S (ΔS, $\Delta M = 0$). The representative matrix can be decomposed into the blocks depending only on the value of S and M. All the anisotropic terms are described by the rank-2 tensor operators which have the non-zero matrix elements between states with $\Delta S = 0, \pm 1, \pm 2$ and their matrices cannot be decomposed into the blocks depending only on the total spin S in account of the S-mixing between spin states with different S. The single-ion anisotropy can be written in terms of the rank-2 single site ITO's [21]. Finally, the antisymmetric exchange term is the sum of the ITO's of the rank-1.

The ITO technique has been used to design the MAGPACK software [23], a package to calculate the energy levels, bulk magnetic properties, and inelastic neutron scattering spectra of the high nuclearity spin clusters that allows studying efficient properties of nanoscopic magnets.

2.1. Calculation of the spin structure of the N-spin system

One of the major challenges in quantum computing is to identify a system that can be scaled up to the number of qubits needed to execute the nontrivial quantum algorithms. Peter Shors algorithm [8] for finding the prime factors of the numbers used in the public-encryption systems (numbers that typically consist of more than a hundred digits) would likely require a quantum computer with e several thousand qubits. Depending on the error correction scheme appropriate to the particular computer, the required number could be much larger. The solid-state spin quantum computers may be more likely candidates. In this work we offer the model of the quantum computer based on studying of the spin structure of the 3d-metal Ni clusters on a silicon surface. In our model the total electronic structure can be written as a sum

of a non-spin-polarized charge, DOS $n_{DOS}(\epsilon)$, and the spin DOS, $S_{DOS}(\epsilon)$,

$$n(\epsilon) = n_{DOS}(\epsilon) + S_{DOS}(\epsilon) \tag{9}$$

The first part $n_{DOS}(\epsilon)$ is connected with a one-electron structure and can be received by any DFT method. The second part $S_{DOS}(\epsilon)$ is purely a spin structure and is defined only proceeding from the spin model of a cluster. In order to separate in the experimental spectra the contributions from a purely spin states and from the excitations connected with the one-electron transitions, is reasonable within an uniform approach to receive the electronic structure of a cluster and then, using the one-electron data for the calculation of the exchange integrals, to calculate the spin structure by the ITO method within the generalized spin Hamiltonian $\widehat{H}_{spin}$. We have developed the idea of spins as a degree of freedom, with which models are built [37]. The spin magnetic moment due to the exchange interaction is

$$\mathbf{M}_s = -2\langle \hat{\mathbf{S}} \rangle \mu_B / \hbar, \tag{10}$$

where

$$\langle \hat{S} \rangle = \sqrt{\left\langle \hat{S}_x \right\rangle^2 + \left\langle \hat{S}_y \right\rangle^2 + \left\langle \hat{S}_z \right\rangle^2}$$

is the spin structure. With the spin-Hamiltonian $\widehat{H}_{spin}$ result (3) we can obtain the quantum mechanical expectation values

$$\langle \hat{S}_x \rangle = \langle SM|\hat{S}_x|SM \rangle, \tag{11}$$

$$\langle \hat{S}_y \rangle = \langle SM|\hat{S}_y|SM \rangle, \tag{12}$$

$$\langle \hat{S}_z \rangle = \langle SM|\hat{S}_z|SM \rangle. \tag{13}$$

With the algebra of the spin operators we can obtain the expectation values for $\widehat{H}_{spin}$

$$\langle \hat{S}_x \rangle = \frac{1}{2} \sum_{\mu=1}^{N} c_\mu^2 A_\mu, \tag{14}$$

$$\langle \hat{S}_y \rangle = -\frac{i}{2} \sum_{\mu=1}^{N} c_\mu^2 B_\mu, \tag{15}$$

$$\langle \hat{S}_z \rangle = \sum_{\mu=1}^{N} c_\mu^2 M^{(\mu)} \tag{16}$$

where

$$A_\mu = \sqrt{S^{(\mu)}(S^{(\mu)}+1) - M^{(\mu)}(M^{(\mu)}+1)}$$

$$+ \sqrt{S^{(\mu)}(S^{(\mu)}+1) - M^{(\mu)}(M^{(\mu)}-1)}$$

and

$$B_\mu = \sqrt{S^{(\mu)}(S^{(\mu)}+1) - M^{(\mu)}(M^{(\mu)}+1)}$$

$$- \sqrt{S^{(\mu)}(S^{(\mu)}+1) - M^{(\mu)}(M^{(\mu)}-1)}$$

The spin DOS $S(\epsilon)$ can be done by inserting the following functions:

$$S_x(\epsilon) = \sum_{\mu=1}^{N} c_\mu^2 A_\mu \delta(\epsilon - \epsilon_\mu), \tag{17}$$

$$S_y(\epsilon) = \sum_{\mu=1}^{N} c_\mu^2 B_\mu \delta(\epsilon - \epsilon_\mu), \tag{18}$$

$$S_z(\epsilon) = \sum_{\mu=1}^{N} c_\mu^2 M^{(\mu)} \delta(\epsilon - \epsilon_\mu). \tag{19}$$

The spin DOS is

$$S_{DOS}(\epsilon) = \sqrt{S_x^2(\epsilon) + S_y^2(\epsilon) + S_z^2(\epsilon)} \tag{20}$$

2.2. Calculation of the magnetic properties

Once we have the energy levels, we can evaluate different thermodynamic properties of the system as the magnetization, the magnetic susceptibility, and the magnetic specific heat. Since in further researches the anisotropic part of GSH will be only scalar, the magnetic properties of the anisotropic system do not depend on the direction of the magnetic field. Thus we can consider the external magnetic field H_z directed along arbitrary axis z of the cluster coordinate frame that is chosen as a spin quantization axis. In this case the energies of the system will be $\epsilon_\mu(M_s) + g_e \beta M_s H_z$, where $\epsilon_\mu(M_s)$ are the eigenvalues of the GSH containing the magnetic exchange and the double exchange contributions (index μ runs over the energy levels with given total spin protection $\mathbf{M}_s$). Then the partition function in the presence of the external magnetic field is given by

$$Z(H_z) = \sum_{M_s,\mu} \exp[-\epsilon_\mu(M_s)/kT] \sum_{M_s} \exp[-g_e \beta M_s H_z/kT] \tag{21}$$

Using this expression one can evaluate the magnetic susceptibility χ and the magnetization M_s by the standard thermodynamic definitions

$$\chi = \left(\frac{\partial \mathbf{M}_s}{\partial \mathbf{H}}\right)_{\mathbf{H}\to 0} \tag{22}$$

$$\mathbf{M}_s(\mathbf{H}) = NkT \frac{\partial \ln Z}{\partial \mathbf{H}} \tag{23}$$

2.3. The spin-dynamics simulations

Broadly speaking, a quantum computer is a physical system that can be initialized to some known state $|\Psi(t_i)\rangle = |\Psi(t_0)\rangle$, and whose dynamics can be controlled so as to induce any unitary transformation of the state vector $|\Psi(t_i)\rangle = \hat{U}|\Psi(t_0)\rangle$. In the standard approach, the computational process is given by the unitary time-evolution operator $\hat{U}$ of the state vector, and is driven by the application of the external stimuli. Under the assumption of a small time step Δt we can expand the time evolution operator

$$\hat{U}(t+\Delta t, t) \approx (I - i\mathcal{H}\Delta t/\hbar) + O(\Delta t^2),$$

where $\widehat{\mathcal{H}} = \widehat{H}_{spin} - i\alpha\widehat{\Gamma}$ with $\widehat{H}_{spin}$ and $\widehat{\Gamma}$ being Hermitian operators and α being a damping constant ($\alpha \geq 0$), leading to the energy dissipation. The dynamic behavior of a spin is determined by the equation of motion, which can be derived from the quantum theory with the spin Hamiltonian $\widehat{H}_{spin}$. This Hamiltonian, which describes the interaction of the spin $\hat{\mathbf{S}}$ with the external magnetic field, given by its flux $\mathbf{H}_{eff}$, can be expressed as

$$\widehat{H}_{spin} = -\mathbf{H}_{eff}\hat{\mathbf{S}} \tag{24}$$

where the effective magnetic field $\mathbf{H}_{eff}$ is an external magnetic field $\mathbf{H}_z$, the anisotropy fields $\mathbf{H}_{an}$, the exchange interaction $\mathbf{H}_{ex}$ and

external magnetic pulse field $\mathbf{H}_{pulse}(t)$. Here we use the approximation for $\mathbf{H}_{eff} \Rightarrow \mathbf{H}_{eff}^{mean}$ with replacement $\hat{\mathbf{S}} \Rightarrow \mathbf{M}_s = \gamma \langle \hat{\mathbf{S}} \rangle$. In [39] it was demonstrated that

$$\frac{\partial \langle \hat{\mathbf{S}} \rangle}{\partial t} = -\langle \hat{\mathbf{S}} \rangle \times \frac{\partial \hat{H}_{spin}}{\partial \langle \hat{\mathbf{S}} \rangle} + \alpha \left(\langle \hat{\mathbf{S}} \rangle \times \frac{\partial \langle \hat{\mathbf{S}} \rangle}{\partial t} \right) \tag{25}$$

This time-dependent equation is similar to the Landau–Lifshitz–Gilbert (LLG) equation [40] for the spin magnetic moment $\mathbf{M}_s$ (10) dynamics

$$\frac{\partial \mathbf{M}_s}{\partial t} = -2\mathbf{M}_s \times \mathbf{H}_{eff}^{mean} + \alpha \mathbf{M}_s \times \frac{\partial \mathbf{M}_s}{\partial t} \tag{26}$$

In order to solve this equation, as an effective magnetic field, we take the variational derivative of the energy with respect to the magnetization

$$\mathbf{H}_{eff}^{mean} = -\frac{\delta \mathfrak{F}}{\delta \mathbf{M}_s}$$

where $\mathfrak{F}$ is the free energy of the magnetic nanosystem

$$\mathfrak{F} = -Nk_B T \ln Z(H_z)$$

with the partition function (21). Here

$$\mathbf{M}_s = -\frac{\partial \mathfrak{F}}{\partial \mathbf{H}}$$

and

$$\chi = \frac{\partial \mathbf{M}_s}{\partial \mathbf{H}},$$

where $\mathbf{H}$ is the magnetic field. Thus

$$\mathbf{H}_{eff}^{mean} = -\frac{\mathbf{M}_s^{(0)}}{\chi^{(0)}}$$

calculated by formulas (22) and (23). We have derived a general form of the time-dependent spin equation for a system of the spins precessing in an effective magnetic field by specifying all the interactions in GSH (3).

2.4. The entanglement in the N-spin system

Identifying and measuring of the entanglement in multi-spin systems presents various complications. Apart from the case of a two-qubit system, where the entanglement can be identified both for a pure and a mixed state [41–44], a multi-qubit entanglement is an open problem [45–47]. For the analysis that follows, we will be using the measure of the recently proposed density of entanglement. Based on the residual entanglement [47], we present the global entanglement of a N-spin state as collective measures of a multi-particle entanglement. These measures were introduced by Meyer and Wallach [48]. The MeyerWallach (MW) measure is written in the Brennen form [49] and we use the Q-measure [48], which corresponds, for a cluster with N qubits, to the average purity of the reduced density matrices of each qubit

$$Q(\psi) = \sum_{k=1}^{N} 2[1 - \mathrm{Tr}(\rho_k^2)] \tag{27}$$

where ρ_k is the reduced density matrix for kth qubit. The problem of the entanglement between spin states in the N-spin systems becomes more interesting when the clusters with a spectral gap in their density of the states are considered. For quantifying the distribution of the entanglement between the individual spin eigenvalues in the spin structure of the N-spin system we use the density of the entanglement (DOE) [50]. The density of entanglement $\varepsilon(\epsilon_\mu, \epsilon_\lambda, \epsilon) \, d\epsilon$ gives the entanglement between the

spin eigenvalue ϵ_μ and the spin eigenvalue ϵ_λ in the energy interval ϵ_μ to $\epsilon_\mu + d\epsilon_\mu$. One can show that the entanglement distribution can be written in terms of a spectrum of a spin excitation

$$S(\epsilon_\lambda, \epsilon) = |c_\lambda|^2 \delta(\epsilon - \epsilon_\lambda) \tag{28}$$

and

$$\varepsilon(\epsilon_\mu, \epsilon_\lambda, \epsilon) = 2S(\epsilon_\lambda, \epsilon)S(\epsilon_\mu, \epsilon) \tag{29}$$

where the coefficient $\langle c_\lambda | SM \rangle$ is the eigenvector (2) of the spin-Hamiltonian (3) of the cluster. Thus, the entanglement distributions can be derived from the excitation spin spectrum

$$Q(\epsilon) = 1 - \frac{2\Delta^2}{\pi^2 N} \sum_{\mu=1}^{N} \frac{|c_\mu|^2}{(\epsilon - \epsilon_\mu)^2 + \Delta^2} \sum_{\lambda=\mu+1}^{N} \frac{|c_\lambda|^2}{(\epsilon - \epsilon_\lambda)^2 + \Delta^2} \tag{30}$$

where Δ is the Lorentzians width. Though the very nature of the entanglement is the purely quantum mechanical, we saw that it can persist for the macroscopic systems and survive even in the thermodynamical limit. In this section we discuss how it behaves at the finite temperature of the thermal entanglement. The states in the N-spin system, describing a system in the thermal equilibrium states, are determined by the generalized spin-Hamiltonian and the thermal density matrix

$$\rho(T) = \frac{\exp(-H_{spin}/kT)}{Z(H_z)} \tag{31}$$

where $Z(H_z)$ is the partition function of the N-spin system. The thermal entanglement is

$$Q(\epsilon, T, H_z) = 1 - \frac{2\Delta^2}{\pi^2 N Z(H_z)^2} \sum_{\mu=1}^{N} \frac{|c_\mu|^2 \exp[-\epsilon_\mu/kT]}{(\epsilon - \epsilon_\mu)^2 + \Delta^2}$$
$$\times \sum_{\lambda=\mu+1}^{N} \frac{|c_\lambda|^2 \exp[-\epsilon_\lambda/kT]}{(\epsilon - \epsilon_\lambda)^2 + \Delta^2} \tag{32}$$

2.5. Calculation of the density of states $n_{DOS}(\epsilon)$

The total density of states $n_{DOS}(\epsilon)$ of Ni$_7$ clusters was calculated by the all-electron density functional theory (DFT) approach implemented in the ADF2013 code [29,30]. The main point of the density functional theory is that the potential acting on each electron of all the other electrons in the molecule or crystal depends only on the electron density of the ground state and its gradient. Thus, we can apply the one-electron formulation of a system of N interacting electrons by introducing the appropriate local exchange–correlation potential $V_{XC}(r)$, in addition to any external potentials $V_{ext}(r)$ and the Coulomb potential of the electron cloud $V_C(r)$ and it has the following form:

$$\left(-\frac{1}{2}\nabla^2 + V_{ext}(\vec{r}) + V_c(\vec{r}) + V_{xc}(\vec{r}) \right) \phi_i(\vec{r}) = \varepsilon_i \phi_i(\vec{r}) \tag{33}$$

The one-electron molecular orbitals ϕ_i with the appropriate orbital energies ε_i define precise electronic charge density and, in principle, give access to all the properties, because they are all expressed in terms of density functional, especially energy. In addition, they allow us to represent the system as a set of independent electron orbitals. In our calculations the electronic configuration of the Ni$_7$ cluster was described by the polarized triple zeta (TZP) basis set of the Slater-type orbitals. The total DOS was obtained using the BLYP exchange functional which is equivalent to Becke (exchange) [31] and Lee–Yang–Parr (LYP correlation) [32]. The calculations were done for the high-spin state of Ni$_7$ cluster.

3. Results and discussion

Here we present the results of the application of our theoretical and experimental approach to study of the N-qubits from seven nickel atoms interacting with a Si (111)-surface in terms of numerically solvable DFT-models for the exchange integrals J_{ij} and we exploit the ITO technique [21] for the calculation of the spin structure of the N-qubits system. In practice, this model was applied to the nanosystem (Ni_7-cluster on Si (111)-surface) and provides an understanding of the chemical bonding of the nickel nanoparticles with the silicon substrate. It is advantageous to have access to sufficiently accurate DFT-total energies to compare the different competing spin configurations. In the most first-principles calculations of the magnetic systems only ferromagnetic or some antiferromagnetic states were considered. Along with these collinear magnetic configurations, many nanomagnetic clusters show the non-collinear ground states, such as conical or spin spirals or commensurate superpositions of several spiral spin-density waves. To access such states from the first principles, the vector-spin DFT, which treats the magnetization density as a vector field (and not as a scalar field as in the collinear DFT calculations), has to be applied [35,36]. The ab initio magnetic interactions are mapped onto a certain parametric GSH model (in the simple cases, the Heisenberg–Dirac–Van Vleck (HDVV) model), which is studied by using the parameters extracted from the microscopic evaluation [13]. Although one of the fundamental parameters is the magnetic moment of the single cluster, ab initio studies of its origin are scarce, so little is known about the cluster spin structure. One of the reasons for the lack of ab initio studies is the number of metal ions as spin sources. The LCAO methods, including the electronic and the spin interactions such as the vector-spin DFT, are applicable for these clusters owing to large number of their active electrons and active spaces, and to the quantum chemical description of the magnetic anisotropy of the nanosystems. Our computations of the electronic and the magnetic properties are based on the LCAO method in the framework of DFT and have been performed with the package SIESTA [53] which was adapted for an investigation of the non-collinear magnetic systems. Starting from the generalized gradient approximation (GGA) for the spin-polarized systems, we apply our on-site constraint method for the systems with the arbitrary magnetic structures to determine the ground state and a set of excited magnetic configurations. To describe the atoms in the SIESTA code, we generated the pseudopotentials for the atomic elements according to the Troullier and Martins procedure [51] with the 3p-semicore states for the Ni atoms. A double-ζ polarized basis set has been used for the Si atoms and a triple-ζ polarized basis set for the Ni atoms. The exchange–correlation functional PBE [52] was employed. For the real space grid, we set a uniform mesh corresponding to an energy cut-off of 200 Ry. We wish to determine the exchange interaction parameters from the first principles by calculating the appropriate total energies and mapping these results onto the Heisenberg model $\hat{H}_{spin}$. The orientational energy dependence (i.e., the dependence of the mutual classical spin orientations) can be interpreted in terms of a classical spin system with an effective spin Hamiltonian. The magnetic state of N atoms can be characterized by the array $\{\mathbf{M}_s^{(i)}\}_{i=1\ldots N}$ where $\mathbf{M}_s^{(i)} = \mu_i \mathbf{S}_i$ is the spin magnetic moment of a particular ion i and μ_i is the magnitude of the magnetic moment. Our calculations result in the values of magnetic moments is $\mu_1 = 1.053\,\mu_B$, $\mu_2 = 0.876\,\mu_B$, $\mu_{3-7} = 0.9\,\mu_B$. In general, the energy of a spin system up to the second order with respect to the spin operators (or the classical spin values) includes the exchange–interaction and the magnetic-anisotropy terms. Since the spinorbital interaction [54] is omitted, the anisotropy terms do not appear in the present
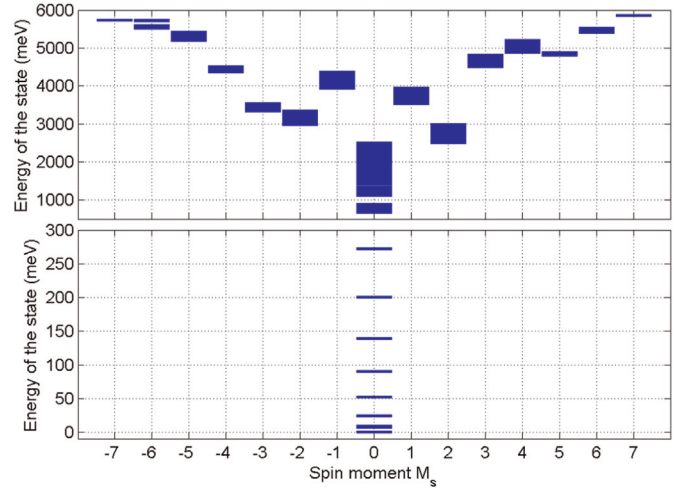

Fig. 1. The anisotropic spin-Hamiltonian spectra of Ni_7 cluster on a silicon surface.

calculations and, therefore, the exchange interaction can be represented solely by the isotropic HDVV term as shown in Eq. (4), where J_{if} is the isotropic exchange coupling constant between spins i and f

$$E(\{\mathbf{S}_i\}, \{J_{if}\}) = \sum_{i>f} J_{if}\,\mathbf{S}_i\cdot\mathbf{S}_f \tag{34}$$

To obtain the exchange coefficients J_{if}, we fit the total energy $E(\{\mathbf{S}_i\}, \{J_{if}\})$ of the spin system, Eq. (35), to the orientational potential relief by using the χ^2 method. For calculation composed of $\hat{H}_{AS}$ and $\hat{H}_{AN}$ in Eq. (3) we used a technique [55].

The calculated (within the GSH model) spin levels of Ni_7 are shown in Fig. 1. They are grouped according to the spin moment M_s. A peculiar feature of the energy pattern is the presence of the levels belonging to $M_s = 0$ (the ground state and the low lying excited states) and $M_s = \pm(1-7)$ (the highly lying excited states) separated by a small gap Δ, and the sets of the excited levels (≥ 300 meV) are well separated from the low-lying levels. The exchange integrals describe the interaction between the spins of the neighboring atoms. From the analysis of the calculated values of the exchange integrals J_{if} of the nickel cluster on a silicon surface it follows that the greatest values 14.2–10.8 meV turn out only for the nearest neighbors further their values sharply decrease (approximately by 3 orders). In this regard our estimates show that the cluster from seven atoms well describes the spin structure of a nickel surface. In our model the total electronic structure can be written as a sum of a non-spin-polarized,charge DOS $n_{DOS}(\epsilon)$, and a spin DOS, $S_{DOS}(\epsilon)$. The spin DOS $S(\epsilon)$ of Ni_7 cluster on a silicon surface is present in Fig. 2. Fig. 3 shows the projected total $n_{DOS}(\epsilon)$ of the Ni_7 cluster calculated without taking into account the relativistic effects. As one can see from the spectrum, there are the free electronic states higher than the LUMO level, which describe well the calculated spin DOS $S(\epsilon)$ of Ni_7 clusters (see Fig. 3).

The comparison of the projected spin DOS $S(\epsilon)$ of Ni_7 cluster on a silicon surface and the one-electron $n_{DOS}(\epsilon)$ of Ni_7 cluster is shown in Fig. 4. In this figure, the Ni 3d-hole one-electron cluster states which coincide with low-lying (0–500 mV) excited spin states have been allocated.

The properties of the 3d-electrons are best probed in an X-ray absorption experiment by the excitation of 2p core electrons to unfilled 3d states. In principle, X-ray absorption spectra contain contributions from both $p \rightarrow d$ and $p \rightarrow s$ transitions, but in practice the $p \rightarrow d$ channel dominates by a factor >20. The line intensities, denoted I_{L_2} and I_{L_3}, respectively, are directly proportional to the number of d holes. The use of circularly polarized X-rays opens the door for spin studies (XMCD spectroscopy). In this
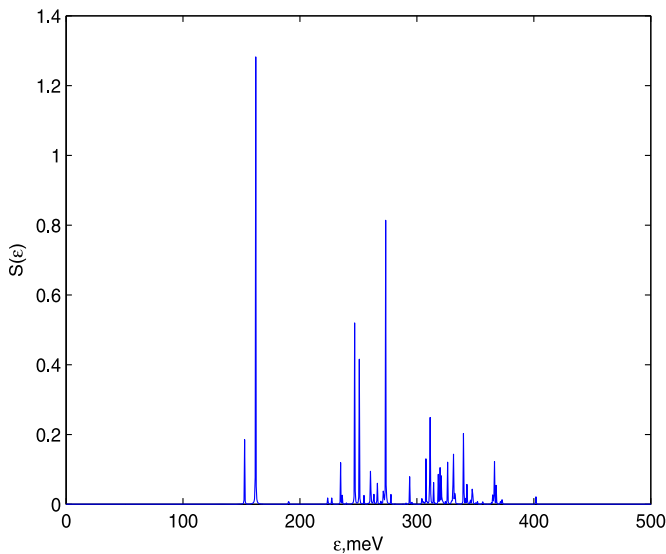
Fig. 2. The projected spin DOS $S(\epsilon)$ of Ni_7 cluster on a silicon (111)-surface.
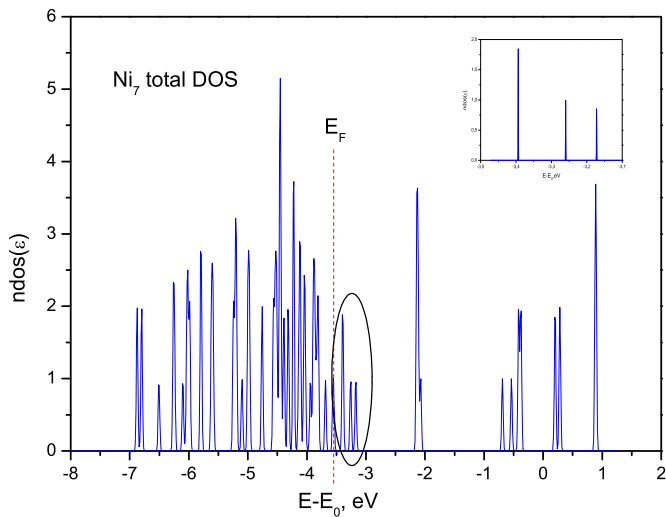

Fig. 3. The projected total one-electron $n_{DOS}(\epsilon)$ of Ni_7 cluster on a silicon surface. Inset: expanded view of the first LUMOs.
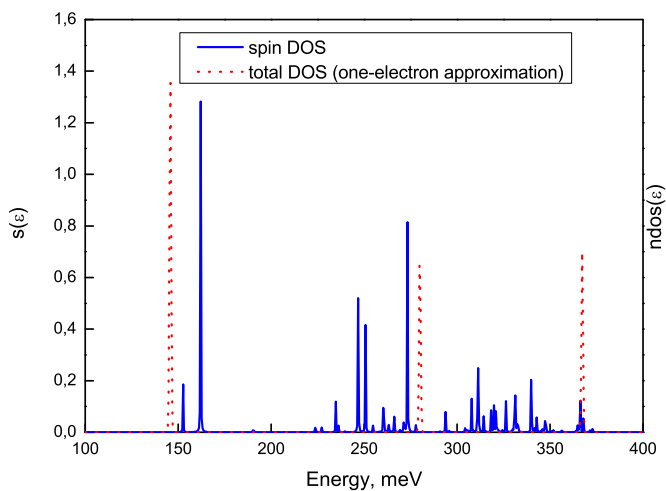

Fig. 4. The comparison of the projected spin DOS $S(\epsilon)$ of Ni_7 cluster on a silicon surface and one-electron $n_{DOS}(\epsilon)$ of Ni_7 cluster.

methodology

$$\mathbf{M}_s = -2\langle \hat{\mathbf{S}} \rangle \mu_B / \hbar = (N_\uparrow - N_\downarrow)\mu_B, \tag{35}$$

where $N_\uparrow$ and $N_\downarrow$ are the numbers of d holes with the spin $\uparrow$ and the spin $\downarrow$, respectively. Now the two-spin model is the main model in XMCD [56]. However it is surprising that the treatment of the X-ray absorption spectra, in general, is based on the simplified model neglecting a mixing of the spin states. Undoubtedly, it would be useful to reconsider interpretation of these spectra, already taking into account mixing of spin states.

In this work X-Ray Absorption Near-Edge Structure (XANES) spectroscopy was used both to study the adsorption geometry and to get information concerning the electronic properties of the deposited Ni-clusters. An interpretation of the experimental XANES data, which were taken from [33], was provided in the present study by model spectra, based on real-space multiple-scattering approach implemented in the FEFF9 program code [27,28]. FEFF9 uses an ab initio self-consistent real space multiple scattering approach, including polarization dependence, core–hole effects, and local field corrections, based on self-consistent, spherical muffin-tin scattering potentials.

In Fig. 5 we show the comparison between the theoretical spectrum, calculated in the one-electron approximation, with the experimental one, taken from [33]. The experimental spectrum was measured for the similar system of Ni clusters grown on the carbon nanotube layer. We have chosen the experimental data as the most suitable for our system Ni clusters on the silicon surface because silicon and carbon atoms have the similar configuration of the electronic shell – $[Ar]ns^2np^3$, where $n=2$ and 3 for carbon and silicon, respectively. As one can see, there are three features on the experimental spectrum called A_1, A_2 and A_3, which represent the spin structure of the Ni clusters. This structure cannot be repeated without taking into account of the multiplet effects. This fact is obvious from the theoretical spectrum calculated by the one-electron FEFF9 code. If we compare the spin DOS $S(\epsilon)$ of Ni_7 cluster on a silicon surface with the post-edge region of the experimental Ni L_3-XANES spectrum for Ni catalyst nanoparticles (see Fig. 6), one can notice that the energy position of the features of spin DOS $S(\epsilon)$ coincides with the post-edge features of the absorption spectrum of Ni clusters.

A studying of the decoherence in the solid-state spin-based qubit systems was the focus of our project. Since the decoherence is a complex many-body non-equilibrium process, and its description by purely analytical means is rarely possible, our main
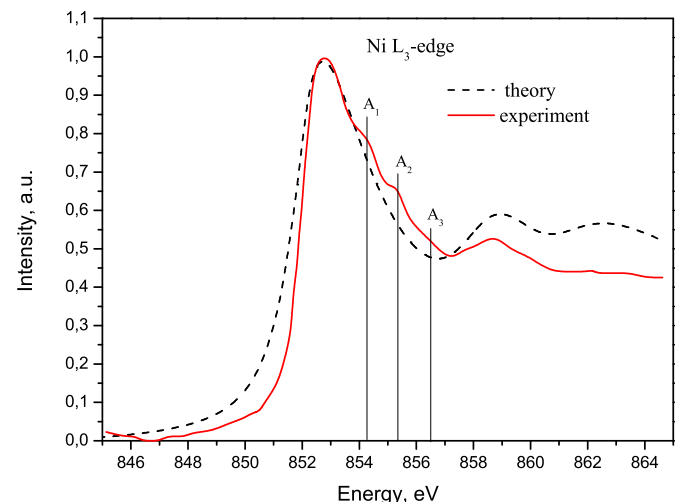

Fig. 5. The theoretical one-electron and experimental NiL_3-edge XANES for Ni_7 cluster on a silicon surface.
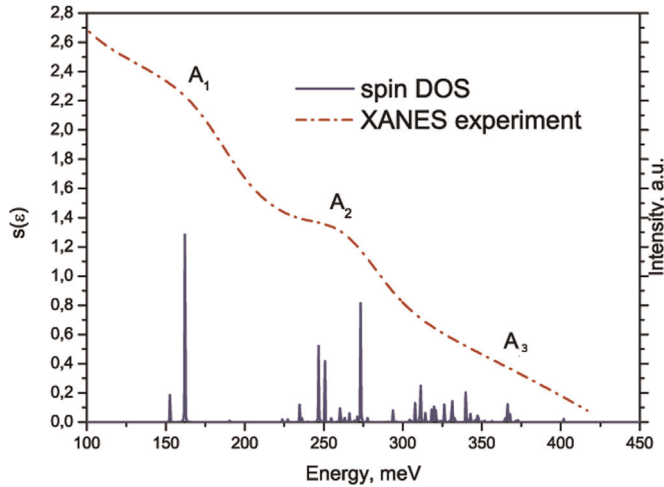
Fig. 6. The comparison of the calculated spin DOS $S(\epsilon)$ of the Ni$_7$ cluster on a silicon surface with the experimental Ni L$_3$-XANES spectra of carbon nanotube with Ni catalyst nanoparticle taken from [26]. The experimental spectrum was shifted on the value of the Ni $2p_{3/2}$ binding energy.

Fig. 7. Time evolution of the quantum mechanical expectation $\langle S \rangle_{x,y,z}$ of Ni$_7$ cluster on a silicon surface ($H_z = 0.01$ Ts).

Fig. 8. Time evolution of the quantum mechanical expectation $\langle S \rangle_{x,y,z}$ of Ni$_7$ cluster on a silicon surface ($H_z = 1.76$ Ts).

tool was the direct and highly accurate numerical solution of the time-dependent Schrödinger equation for the whole system (qubits plus their silicon substrate). This is very difficult but extremely reliable approach, involving no approximations about a system or a environment. In this study we have developed and used the advanced numerical techniques to accurately assess the details of the decoherence process governing the dynamics of SSNQ interacting with a silicon surface. A well-studied model for the decoherence is a central-spin system coupled to the N noninteracting spins. The exact evaluation of dynamics for the central spins is obtained for the special cases, where there is uniform coupling with the spin bath, or a special choice of the initial states, or the system–bath interaction is a simple interaction between the z-component of the spins. Each such studied case can explain the experimentally observed results in some solid-state devices. We offer a model in which there is no division of the Hamiltonian on H_0 and H_{bath}, and the interaction with a bath (environment) is considered in the GSH technique at the calculation of the exchange integrals J_{ij} of a nanosystem Ni$_7$–Si in the one-electron approach taking into account the chemical bonds of all atoms of the Si substrate (environment) with the atoms of the Ni$_7$ cluster. We investigated in detail the electron spin decoherence and Rabi oscillations for various magnetic fields H_z. As a result, we developed a new method of simulations of the decoherence, which allowed modeling of the realistically large systems (thousands of quantum spins) with a complex dynamics. Here we used 2187 spins for the generalized spin Hamiltonian. A noticeable part of our studies has become possible due to the progress in the methods for a numerical modeling of a decoherence. We also studied the visibility and the decay of Rabi oscillations in SSNQ qubits. In Fig. 7 we have plotted the Rabi oscillations to evaluate the qubit as a function of the time and $H_z = 0.01$ Ts. An important requirement for a quantum computing is a control, which can be made through the magnetic fields. In Fig. 8 we have plotted the Rabi oscillations to evaluate the qubit as a function of the time and $H_z = 1.76$ Ts. Here we show the quantum state stabilization (stabilizing Rabi oscillations) in the Ni$_7$–Si nanosystem for $H_z = 1.76$ Ts. Thus, we have observed the stabilized Rabi oscillations and the stabilized quantum dynamical qubit state and the Rabi driving after the fixed time (0.327 μs).

Today, in fact, the quantum entanglement is recognized as a new physical resource which is important for a quantum computation. We have analyzed a behavior of the entanglement in the
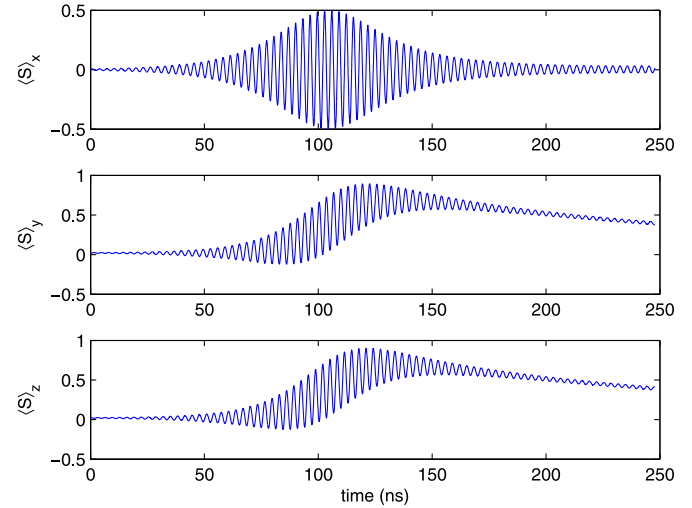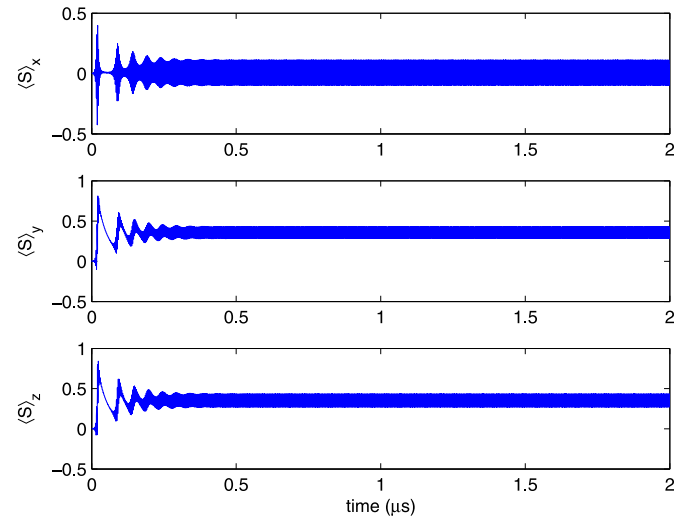
finite clusters of the quantum spins and have shown that the entanglement in these systems is significantly modified near special values of the energy and temperature. These results could be particularly relevant for applications in quantum computations. In this paper we have identified the global entanglement patterns in SSNQ by analyzing the behavior of the density of entanglement as a function of the energy and temperature, which ultimately leads to a change in the spin structure of the cluster.

Identifying and measuring entanglement in the multi-spin systems is a challenge. Apart from the case of a two-qubit system, where an entanglement can be identified both for a pure and a mixed state [41–44], the multi-qubit entanglement is an open problem and to date several measures of an entanglement have been proposed [45–47]. For the analysis that follows we will be using the global entanglement [47] since this will enable us to deal with many spin eigenvalues (spin modes). Since we will assume only a single excitation in each cluster spin mode, we can treat the cluster spin states as a set of qubits for the purpose of computing global entanglement. For quantifying the distribution of an entanglement between the individual spin eigenvalues in the spin structure of the SSNQ-system in a Ni$_7$-cluster on a silicon substrate we use the density of entanglement. In Fig. 9 we have plotted the
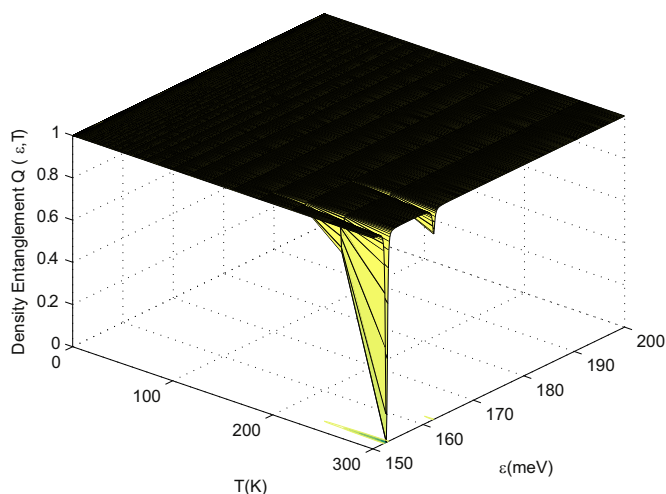
Fig. 9. The calculated density of global entanglement vs. temperature and energy for Ni_7 cluster on a silicon surface.

calculated density of the global entanglement vs. temperature and energy for the Ni_7 cluster on a silicon surface. From the figure we can see that in the wide interval of the temperatures from 0 to 230 K and in the range of the energy from 0 to 200 meV practically all states of SSNQ have the most entanglement that is very important for the work of the quantum computer. Since 230 K at the energy $\epsilon_1 = 153$ meV and $\epsilon_2 = 162$ meV there is a sharp falling of a complexity and we observed the spectral gap in DOE. In this context, the systematic studies of the relationship between the amount and nature of an entanglement and a spin structure have been pursued in order to the identify optimal researches to create specific types of the entanglements.

4. Concluding remarks

Under technological inputs, the cluster magnetism is now moving more and more towards surface science with the implications for the use of new theoretical and experimental techniques and with the development of new synthetic approaches. The cluster nanomagnets on a nonmagnet substrate have specific features that make them paradigmatic cases to the test models and with which we may build the novel quantum architectures. Carrying out a theoretical and experimental investigation of the quantum model of the solid-state spin qubit Ni on a nonmagnetic silicon surface for the quantum register, the quantum computer theory is developed. Within the present paper, we used the numerical simulations and X-ray spectral methodology to study of a spin structure, micromagnetic simulations decoherence and a global density of entanglement in the N-spin qubit systems. We have also investigated important fundamental problems of an entanglement and a decoherence theory in the N-spin nanosystem Ni3d–Si heterostructure. We have studied the spin structure, the dynamics of decoherence vs. magnetic field and the global entanglement in the hybrid nanosystems. As a result, we have provided the detailed theoretical and experimental description for many important aspects of the spin structure, the decoherence and the entanglement in the systems relevant for quantum information processing and quantum computers. No doubt, the challenges we face in building a real silicon-based N-qubit with $N \geq 2000$ are significant, but our initial results offer hope that large-scale quantum computing may one day be realized.

References

[1] M.A. Nielsen, I.L. Chuang, Quantum Computation and Quantum Information, Cambridge University Press, Cambridge, New York, 2000.
[2] D. Loss, D.P. DiVincenzo, Phys. Rev. A 57 (1998) 120.
[3] G. Burkard, D. Loss, D.P. Di Vincenzo, Phys. Rev. B 59 (1999) 2070.
[4] B.E. Kane, Nature 393 (1998) 133.
[5] J. Wrachtrup, F. Jelezko, J.Phys.: Condens. Matter 18 (2006) 807.
[6] L. Childress, M.V. Gurudev, J.M. Taylor, Science 314 (2006) 281.
[7] X.-G. Li, J.N. Fry, H.-P. Cheng, Phys. Rev. B 90 (2014) 125447.
[8] P. Shor, in: Proceedings of the 35th Annual Symposium on Foundations of Computer Science, 1994, pp. 116–123.
[9] K. Wu, B. Zhou, W. Cao, Phys. Lett. A 362 (2007) 381.
[10] G. Wolfowicz, A.M. Tyryshkin, R.E. George, H. Riemann, N.V. Abrosimov, P. Becker, H.-J. Pohl, M.L.W. Thewalt, S.A. Lyon, J.J.L. Morton, Nat. Nanotechnol. 8 (2013) 561.
[11] F. Troiania, M. Affronte, Chem. Soc. Rev. 40 (2011) 3119.
[12] O.O. Brovko, O.V. Farberovich, V.S. Stepanyuk, J. Phys.: Condens. Matter 26 (2014) 315010.
[13] V.V. Maslyuk, I. Mertig, O.V. Farberovich, A. Tarantul, B. Tsukerblat, Eur. J. Inorg. Chem. 2013 (2013) 1897.
[14] W. Zhang, N. Konstantinidis, K.A. Al-Hassanieh, V.V. Dobrovitski, J. Phys.: Condens. Matter 19 (2007) 083202.
[15] K.A. Al-Hassanieh, V.V. Dobrovitski, E. Dagotto, B.N. Harmon, Phys. Rev. Lett. 97 (2006) 037204.
[16] W. Zhang, K.A. Al-Hassanieh, V.V. Dobrovitski, E. Dagotto, B.N. Harmon, Phys. Rev. B 74 (2006) 205313.
[17] R. Horodecki, P. Horodecki, M. Horodecki, K. Horodecki, Rev. Mod. Phys. 81 (2009) 865.
[18] L. Amico, R. Fazio, A. Osterloh, V. Vedral, Rev. Mod. Phys. 80 (2008) 517.
[19] G.L. Kamta, A.F. Starace, Phys. Rev. Lett. 88 (2002) 107901.
[20] C.H. Bennett, D. DiVincenzo, Nature 404 (2012) 247.
[21] J.J. Borras-Almenar, J.M. Clemente-Juan, E. Coronado, B.S. Tsukerblat, Inorg. Chem. 38 (1999) 6081.
[22] X.-Z. Yuan, H.-S. Goan, K.-D. Zhu, N. J. Phys. 13 (2011) 023018.
[23] J.J. Borras-Almenar, J.M. Clemente-Juan, E. Coronado, B.S. Tsukerblat, J. Comput. Chem. 22 (2001) 985.
[24] G. Lagmago Kamta, A.Y. Istomin, A.F. Starace, Eur. Phys. J. D 44 (2007) 389.
[25] V.L. Mazalova, A.A. Guda, N.Yu. Smolentsev, O.E. Polozhentsev, I.G. Alperovich, A.V. Soldatov, S.P. Lau, X.H. Ji, in: I.A. Parinov (Ed.), Piezoelectrics and Related Materials, Nova Science Pub Inc., New York, USA, 2012, pp. 51–77.
[26] V. Mazalova, A. Soldatov, R. Johnston, A. Yakovlev, T. Moller, S. Adam, J. Phys. Chem. C 113 (2009) 9086.
[27] J.J. Rehr, J.J. Kas, F.D. Vila, M.P. Prange, K. Jorissen, J. Phys. Chem. 12 (2010) 5503.
[28] J.J. Rehr, J.J. Kas, M.P. Prange, A.P. Sorini, Y. Takimoto, F.D. Vila, C. R. Phys. 10 (2009) 548.
[29] G. te Velde, F.M. Bickelhaupt, S.J.A. van Gisbergen, C. Fonseca Guerra, E. J. Baerends, J.G. Snijders, T. Ziegler, J. Comput. Chem. 22 (2001) 931.
[30] C. Fonseca Guerra, J.G. Snijders, G. te Velde, E.J. Baerends, Theor. Chem. Acc. 99 (1998) 391.
[31] A.D. Becke, Phys. Rev. A 38 (1988) 3098.
[32] C. Lee, W. Yang, R.G. Parr, Phys. Rev. B 37 (1988) 785.
[33] J. Gao, J. Zhong, L. Bai, J. Liu, G. Zhao, X. Run, Sci. Rep. 4 (2013) 3606.
[34] D.W. Boukhvalov, V.V. Dobrovitski, M.I. Katsnelson, A.I. Lichtenstein, B. N. Harmon, P. Kögerler, Phys. Rev. B 70 (2004) 054417.
[35] J. Kübler, K.-H. Höck, J. Sticht, A.R. Williams, J. Phys. F 18 (1988) 469.
[36] V.V. Maslyuk (Ph.D. thesis), Simulation of the electronic transport through organometallic molecules. Martin Luther University of Halle-Wittenberg, 2009.
[37] D. Loss, D.P. DiVincenzo, Phys. Rev. A 57 (1998) 120.
[39] R. Wieser, Phys. Rev. Lett. 110 (2013) 147201.
[40] R. Wieser, E.Y. Vedmedenko, R. Wiesendanger, Phys. Rev. Lett. 106 (2011) 067204.
[41] W.K. Wootters, Phys. Rev. Lett. 80 (1998) 2245.
[42] A. Uhlmann, Phys. Rev. A 62 (2000) 032307.
[43] K. Audenaert, F. Verstraete, De Moor, Phys. Rev. A 64 (2001) 052304.
[44] W.K. Wootters, Quantum Inf. Comput. 1 (2001) 27.
[45] V. Coffman, J. Kundu, W.K. Wootters, Phys. Rev. A 61 (2000) 052306.
[46] A. Wong, N. Christensen, Phys. Rev. A 63 (2001) 044301.
[47] C.-S. Yu, H. Song, Phys. Rev. A 71 (2005) 044301.
[48] D.A. Meyer, N.R. Wallach, J. Math. Phys. 43 (2002) 4273.
[49] G.K. Brennen, Quant. Inf. Comput. 3 (2003) 619.
[50] C. Lazarou, B.M. Garraway, J. Piilo, S. Maniscalco, J. Phys. B: Atom. Mol. Opt. Phys. 44 (2011).
[51] N. Troullier, J.L. Martins, Phys. Rev. B 1991 (1993) 43.

[52] J.P. Perdew, K. Burke, M. Ernzerhof, Phys. Rev. Lett. 77 (1996) 3865.
[53] D. Sanchez-Portal, P. Ordejon, E. Artacho, J.M. Soler, Int. J. Quantum Chem. 65 (1997) 453.
[54] J. Kortus, M.R. Pederson, T. Baruah, N. Bernstein, C.S. Hellberg, Polyhedron 22 (2003) 1871.

[55] S. Bornemann, O. Sipr, S. Mankovsky, S. Polesya, J.B. Staunton, W. Wurth, H. Ebert, J. Minar, Phys. Rev. B 86 (2012) 104436.
[56] J. Stöhr, J. Magn. Magn. Mater. 200 (1999) 470.